



Received 6 January 2025

Accepted 8 January 2025

Edited by X. Hao, Institute of Chemistry, Chinese Academy of Sciences

Keywords: crystal structure; non-covalent interactions; hydrogen bond.**CCDC references:** 2415427; 2415426**Supporting information:** this article has supporting information at journals.iucr.org/e

Syntheses, crystal structures, Hirshfeld surface analyses and crystal voids of 1-(4-bromophenyl)-2,2-dichloroethan-1-one and 2,2-dibromo-1-(*p*-tolyl)ethan-1-one

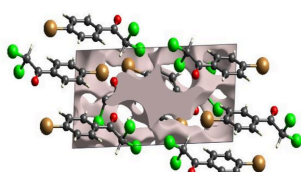
Atash V. Gurbanov,^{a,b} Firudin I. Guseinov,^{c,d} Aida I. Samigullina,^d Tuncer Hökelek,^e Khudayar I. Hasanov,^f Tahir A. Javadzade^g and Alebel N. Belay^{h*}

^aExcellence Center, Baku State University, Z. Xalilov Str. 23, AZ 1148 Baku, Azerbaijan, ^bCentro de Quimica Estrutural, Instituto Superior Tecnico, Universidade de Lisboa, Av. Rovisco Pais, 1049-001 Lisbon, Portugal, ^cKosygin State University of Russia, 117997 Moscow, Russian Federation, ^dN. D. Zelinsky Institute of Organic Chemistry, Russian Academy of Sciences, 119991 Moscow, Russian Federation, ^eHacettepe University, Department of Physics, 06800 Beytepe-Ankara, Türkiye, ^fAzerbaijan Medical University, Scientific Research Centre (SRC), A. Kasumzade Str. 14, AZ 1022 Baku, Azerbaijan, ^gDepartment of Chemistry and Chemical Engineering, Khazar University, Mahzati Str. 41, AZ 1096 Baku, Azerbaijan, and ^hDepartment of Chemistry, Bahir Dar University, PO Box 79, Bahir Dar, Ethiopia. *Correspondence e-mail: alebel.nibret@bdu.edu.et

The asymmetric units of the compounds, C₈H₅BrCl₂O (I), and C₉H₈Br₂O (II), contain two and one crystallographically independent molecules, respectively. In compound (I), the planar rings are oriented at a dihedral angle of 13.23 (8)[°]. In crystals of both compounds, intermolecular C—H···O hydrogen bonds link the molecules into infinite chains along the *b*-axis direction. In crystal of (I), there are π–π interactions between the centroids of the parallel rings with centroid-to-centroid distances of 3.5974 (14), 3.6178 (16) and 3.9387 (16) Å while neither π–π nor C—H···π(ring) interactions are present in (II). The Hirshfeld surface analyses of the crystal structures indicate that the most important contributions for the crystal packings are from H···Cl/Cl···H (27.5%), H···O/O···H (15.0%), H···Br/Br···H (10.2%) and H···H (9.0%) for (I) and H···Br/Br···H (36.1%), H···H (22.2%), H···O/O···H (14.1%) and H···C/C···H (13.9%) for (II). Hydrogen bonding and van der Waals interactions are the dominant interactions in the crystal packings. The volumes of the crystal voids and the percentages of free spaces in the unit cells were calculated to 111.55 Å³ and 12.27% for (I) and 63.37 Å and 6.69% for (II), showing that no large cavities are present in either structure.

1. Chemical context

α-Haloketones are useful synthetic building blocks for the syntheses of pharmacologicals as well as complex organic molecules (Erian *et al.*, 2003). In fact, the existence of two adjacent electrophilic centres, namely the α-halocarbon and carbonyl group, transforms these reactive carbonyl compounds into highly valuable building blocks for the construction of more complex structures (Guseinov *et al.*, 2006, 2017, 2020; Khalilov *et al.*, 2024). Over the past few decades, substantial advances have been made in the syntheses of these industrially relevant building blocks and synthetic precursors (Ma *et al.*, 2021; Mahmoudi *et al.*, 2017; Mizar *et al.*, 2012). Efforts have focused on rendering the synthetic protocols greener, more effective and versatile. Not only electron-withdrawing properties, but the halogen-bond-donor ability of the halogen atom(s) of α-haloketones can dictate their reactivity and other functional properties (Gurbanov *et al.*, 2022). For instance, recently we showed that the reaction of α,α-dihalo-β-oxoaldehydes with diaminofuranan at room



OPEN ACCESS

Published under a CC BY 4.0 licence

Table 1Hydrogen-bond geometry (\AA , $^\circ$) for (I).

$D-\text{H}\cdots A$	$D-\text{H}$	$\text{H}\cdots A$	$D\cdots A$	$D-\text{H}\cdots A$
C1A—H1A \cdots O2B ^{viii}	1.00	2.18	3.100 (3)	152
C1B—H1B \cdots O2A ^{vi}	1.00	2.18	3.166 (3)	169
C8A—H8A \cdots O2B ^{viii}	0.95	2.47	3.374 (3)	160

Symmetry codes: (vi) $x + 1, y, z$; (viii) $x, y - 1, z$.**Table 2**Hydrogen-bond geometry (\AA , $^\circ$) for (II).

$D-\text{H}\cdots A$	$D-\text{H}$	$\text{H}\cdots A$	$D\cdots A$	$D-\text{H}\cdots A$
C1—H1 \cdots O2 ⁱⁱ	1.00	2.20	3.173 (4)	165
C8—H8 \cdots O2 ⁱⁱ	0.95	2.51	3.403 (3)	157

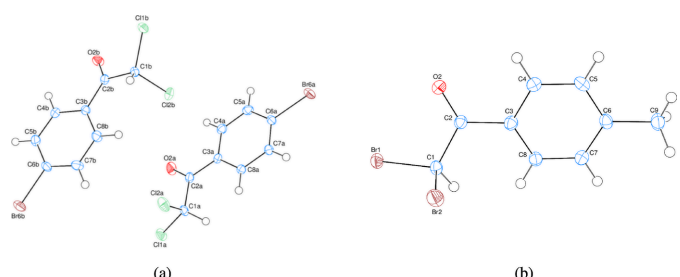
Symmetry code: (ii) $-x + 2, y - \frac{1}{2}, -z + \frac{3}{2}$.

temperature in an acetonitrile solution yields 20-membered macrocycles and *N*-(4-amino-1,2,5-oxadiazol-3-yl)formamide (Guseinov *et al.*, 2024). Herein, we found that when this reaction is carried out in a chloroform solution and at 353 K, both α -haloketones namely 1-(4-bromophenyl)-2,2-dichloroethan-1-one (I) and 2,2-dibromo-1-(*p*-tolyl)ethan-1-one (II) and *N*-(4-amino-1,2,5-oxadiazol-3-yl) formamide are formed. Herein, we have report on the syntheses and molecular and crystal structures of compounds (I) and (II) together with analyses of the Hirshfeld surfaces and crystal voids.

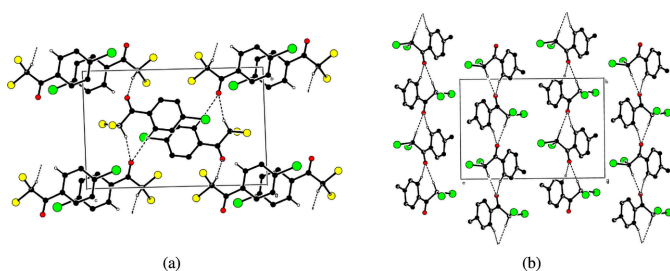


2. Structural commentary

The asymmetric units of compounds (I) and (II) contains two and one crystallographically independent molecules, respectively (Fig. 1). In compound (I), the planar, *A* (C3A–C8A) and *B* (C3B–C8B) rings are oriented at a dihedral angle of 13.23 (8) $^\circ$. Atoms Br6A, C2A, C1A, O2A and Br6B and C2B are 0.0116 (3), 0.023 (3), −0.004 (3), 0.045 (2) \AA and −0.0083 (3), −0.032 (3) \AA , respectively, away from the best least-squares planes of the *A* and *B* rings. In compound (II), atoms Br1, C2 and C9 are 0.0426 (3), 0.058 (3) and 0.041 (3) \AA , respectively, away from the best least-squares

**Figure 1**

The asymmetric units of compounds (a) (I) and (b) (II) with atom-numbering schemes and 50% probability ellipsoids.

**Figure 2**

Partial packing diagrams for compounds (a) (I) and (b) (II). Intermolecular C—H \cdots O hydrogen bonds are shown as dashed lines. H atoms not involved in these interactions have been omitted for clarity.

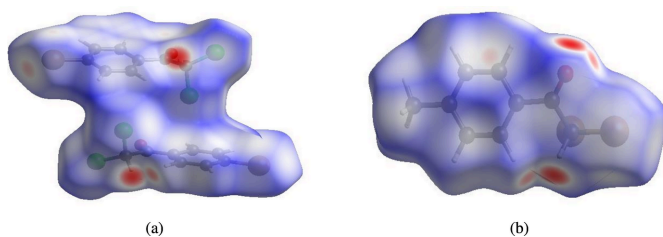
plane of ring *A* (C3–C8). All bond lengths and angles are normal in both compounds.

3. Supramolecular features

In the crystals of both compounds, intermolecular C—H \cdots O hydrogen bonds (Tables 1 and 2) link the molecules into infinite chains along the *b*-axis direction (Fig. 2). In crystal of (I), there are π — π interactions between the centroids of parallel *A* (C3A–C8A) rings and parallel *B* (C3B–C8B) rings with centroid-to-centroid distances of 3.5974 (14) \AA for the *A* rings and 3.6178 (16) and 3.9387 (16) \AA for the *B* rings. No such interactions occur in (II).

4. Hirshfeld surface analysis

In order to visualize the intermolecular interactions in the title compounds, Hirshfeld surface (HS) analyses (Hirshfeld, 1977; Spackman & Jayatilaka, 2009) were carried out using *Crystal Explorer* 17.5 (Spackman *et al.*, 2021). In the HS plotted over d_{norm} (Fig. 3a and b), the white surfaces indicate contacts with distances equal to the sum of van der Waals radii, and the red and blue colours indicate distances shorter (in close contact) or longer (distinct contact) than the van der Waals radii, respectively (Venkatesan *et al.*, 2016). The bright-red spots indicate their roles as donors and/or acceptors; they also appear as blue and red regions corresponding to positive and negative potentials on the HS mapped over electrostatic potential (Spackman *et al.*, 2008; Jayatilaka *et al.*, 2005), as shown in Fig. 4 for compound (II). The π — π stacking interactions were further visualized by plotting the shape-index

**Figure 3**

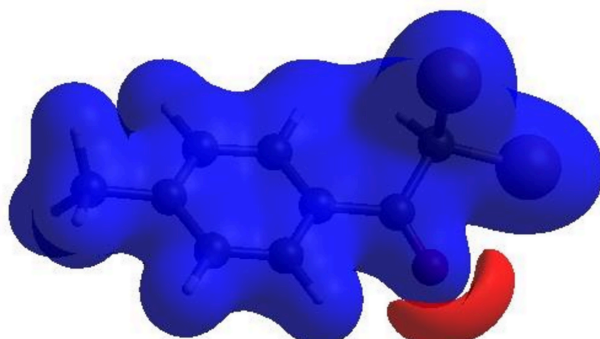
Views of the three-dimensional Hirshfeld surfaces of compounds (a) (I) and (b) (II) plotted over d_{norm} .

Table 3Selected interatomic distances (\AA) for (I).

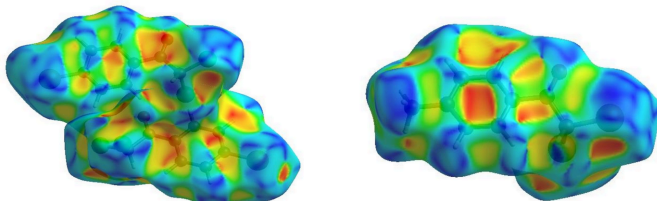
$\text{Br}_6A \cdots \text{Br}_6B^i$	3.4966 (4)	$\text{H}5B \cdots \text{O}2A^{vii}$	2.63
$\text{Br}_6A \cdots \text{Cl}1A^{ii}$	3.554 (3)	$\text{O}2A \cdots \text{H}4A$	2.50
$\text{C}2A \cdots \text{Br}6A^{ii}$	3.515 (3)	$\text{O}2B \cdots \text{H}1A^v$	2.18
$\text{Br}_6B \cdots \text{C}2B^{iii}$	3.504 (2)	$\text{O}2B \cdots \text{H}4B$	2.52
$\text{Br}_6A \cdots \text{H}1A^{ii}$	3.03	$\text{O}2B \cdots \text{H}8A^v$	2.47
$\text{Cl}1A \cdots \text{O}2A$	2.894 (2)	$\text{C}6A \cdots \text{C}8A^{ii}$	3.361 (3)
$\text{Cl}1B \cdots \text{O}2B$	2.901 (2)	$\text{C}1A \cdots \text{H}8A$	2.61
$\text{Cl}2B \cdots \text{C}8B$	3.453 (3)	$\text{C}1B \cdots \text{H}8B$	2.62
$\text{Cl}2B \cdots \text{C}4A$	3.251 (3)	$\text{C}8A \cdots \text{H}1A$	2.63
$\text{Cl}2B \cdots \text{H}8B$	2.88	$\text{C}8B \cdots \text{H}1B$	2.67
$\text{O}2A \cdots \text{C}1B^{iv}$	3.166 (3)	$\text{H}1A \cdots \text{H}8A$	2.06
$\text{O}2B \cdots \text{C}1A^v$	3.100 (3)	$\text{H}1B \cdots \text{H}8B$	2.20
$\text{H}1B \cdots \text{O}2A^{vi}$	2.18		

Symmetry codes: (i) $x, y, z - 1$; (ii) $-x + 1, -y + 1, -z + 1$; (iii) $-x + 2, -y + 2, -z + 2$; (iv) $x - 1, y, z$; (v) $x, y + 1, z$; (vi) $x + 1, y, z$; (vii) $-x + 1, -y + 2, -z + 2$.

surface, which can be used to identify characteristic packing modes, in particular, planar stacking arrangements and the presence of aromatic stacking interactions such as $\text{C}-\text{H} \cdots \pi$ and $\pi-\pi$ interactions. $\text{C}-\text{H} \cdots \pi$ interactions would be seen as red *p*-holes, which are related to the electron ring interactions between the CH groups with the centroids of the aromatic rings of neighbouring molecules. Fig. 5 clearly suggests that there are no $\text{C}-\text{H} \cdots \pi$ interactions in either compound. On the other hand, the shape-index of the HS is also a tool for visualizing $\pi-\pi$ stacking by the presence of adjacent red and blue triangles; if there are no adjacent red and/or blue triangles, then there are no $\pi-\pi$ interactions. Fig. 5 clearly suggests that there are $\pi-\pi$ interactions in compound (I) only.

**Figure 4**

View of the three-dimensional Hirshfeld surface of compound (II) plotted over electrostatic potential energy using the STO-3 G basis set at the Hartree–Fock level of theory. Hydrogen-bond donors and acceptors are shown as the blue and red regions around the atoms corresponding to positive and negative potentials, respectively.

**Figure 5**

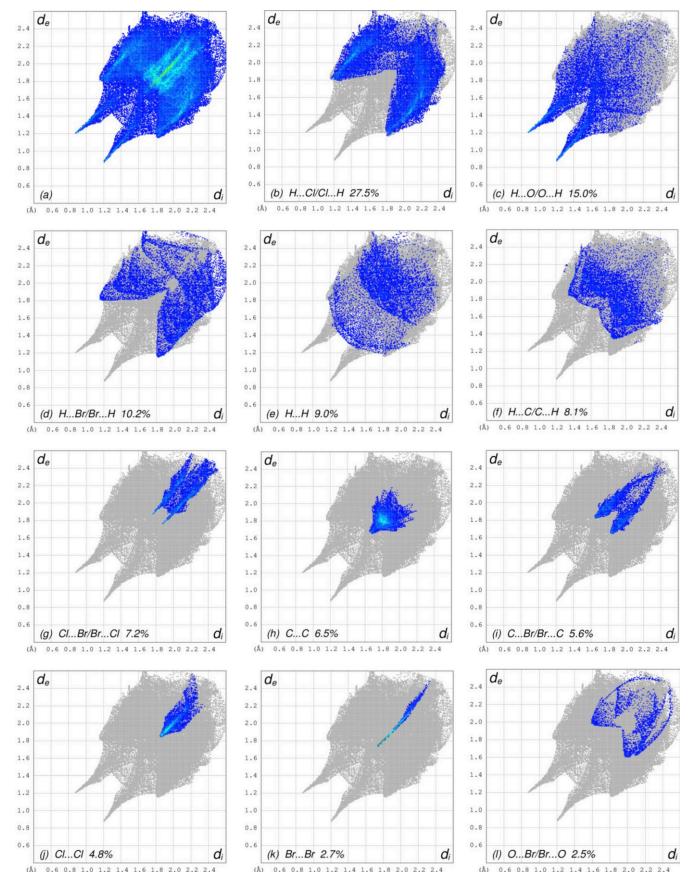
Hirshfeld surfaces of compounds (a) (I) and (b) (II) plotted over shape-index.

Table 4Selected interatomic distances (\AA) for (II).

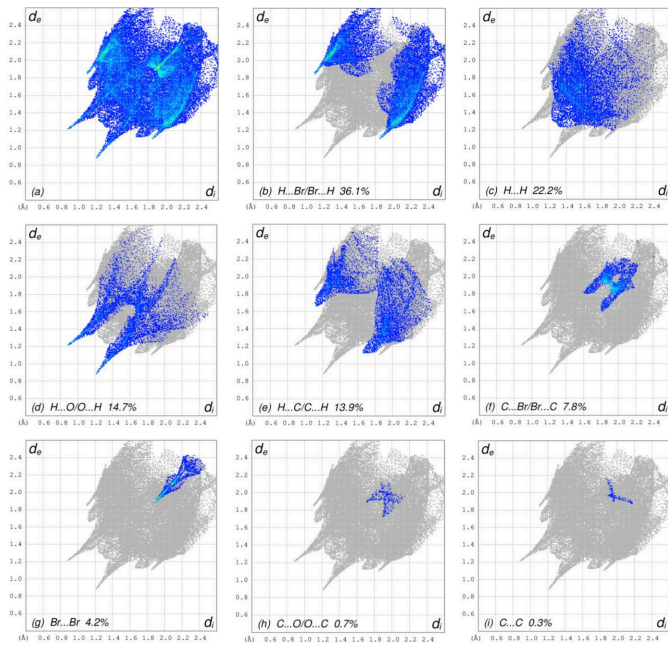
$\text{Br}1 \cdots \text{O}2$	3.011 (2)	$\text{H}8 \cdots \text{O}2^{ii}$	2.51
$\text{C}4 \cdots \text{Br}2^i$	3.452 (3)	$\text{C}1 \cdots \text{H}8$	2.67
$\text{C}5 \cdots \text{Br}2^i$	3.534 (3)	$\text{C}8 \cdots \text{H}1$	2.62
$\text{C}1 \cdots \text{O}2^{ii}$	3.173 (4)	$\text{H}1 \cdots \text{H}8$	2.03
$\text{O}2 \cdots \text{H}4$	2.53	$\text{H}5 \cdots \text{H}9C$	2.40
$\text{H}1 \cdots \text{O}2^{ii}$	2.20		

Symmetry codes: (i) $x, -y + \frac{3}{2}, z + \frac{1}{2}$; (ii) $-x + 2, y - \frac{1}{2}, -z + \frac{3}{2}$.

The overall two-dimensional fingerprint plots (McKinnon *et al.*, 2007) [Fig. 6*a* for (I) and Fig. 7*a* for (II)], and those delineated into $\text{H} \cdots \text{Cl}/\text{Cl} \cdots \text{H}$, $\text{H} \cdots \text{O}/\text{O} \cdots \text{H}$, $\text{H} \cdots \text{Br}/\text{Br} \cdots \text{H}$, $\text{H} \cdots \text{H}$, $\text{H} \cdots \text{C/C} \cdots \text{H}$, $\text{Cl} \cdots \text{Br}/\text{Br} \cdots \text{Cl}$, $\text{C} \cdots \text{C}$, $\text{C} \cdots \text{Br}/\text{Br} \cdots \text{C}$, $\text{Cl} \cdots \text{Cl}$, $\text{Br} \cdots \text{Br}$, $\text{O} \cdots \text{Br}/\text{Br} \cdots \text{O}$, $\text{C} \cdots \text{Cl}/\text{Cl} \cdots \text{C}$ and $\text{O} \cdots \text{Cl}/\text{Cl} \cdots \text{O}$ interactions for (I) and $\text{H} \cdots \text{Br}/\text{Br} \cdots \text{H}$, $\text{H} \cdots \text{H}$, $\text{H} \cdots \text{O}/\text{O} \cdots \text{H}$, $\text{H} \cdots \text{C/C} \cdots \text{H}$, $\text{C} \cdots \text{Br}/\text{Br} \cdots \text{C}$, $\text{Br} \cdots \text{Br}$, $\text{C} \cdots \text{O}/\text{O} \cdots \text{C}$ and $\text{C} \cdots \text{C}$ interactions for (II) are illustrated in Fig. 6*b–n* and Fig. 7*b–i*, respectively, together with their relative contributions to the Hirshfeld surfaces. The most important interactions (Tables 3 and 4) are $\text{H} \cdots \text{Cl}/\text{Cl} \cdots \text{H}$ for (I) and $\text{H} \cdots \text{Br}/\text{Br} \cdots \text{H}$ for (II).

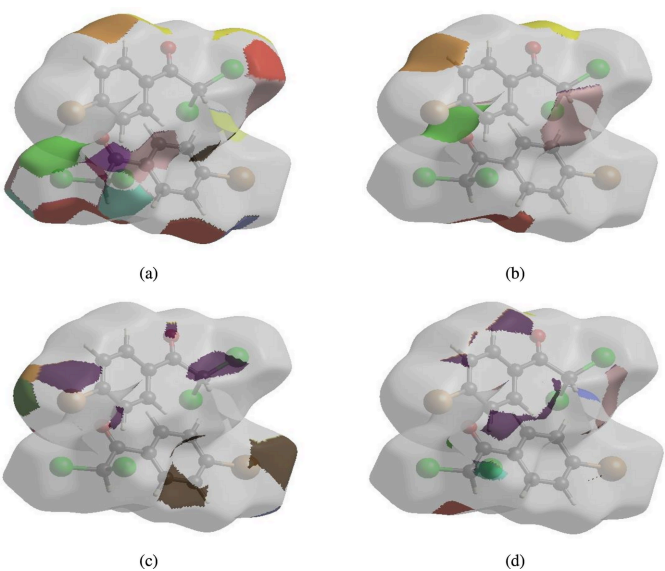
**Figure 6**

The full two-dimensional fingerprint plots for compound (I), showing (a) all interactions, and delineated into (b) $\text{H} \cdots \text{Cl}/\text{Cl} \cdots \text{H}$, (c) $\text{H} \cdots \text{O}/\text{O} \cdots \text{H}$, (d) $\text{H} \cdots \text{Br}/\text{Br} \cdots \text{H}$, (e) $\text{H} \cdots \text{H}$, (f) $\text{H} \cdots \text{C/C} \cdots \text{H}$, (g) $\text{Cl} \cdots \text{Br}/\text{Br} \cdots \text{Cl}$, (h) $\text{C} \cdots \text{C}$, (i) $\text{C} \cdots \text{Br}/\text{Br} \cdots \text{C}$, (j) $\text{Cl} \cdots \text{Cl}$, (k) $\text{Br} \cdots \text{Br}$, (l) $\text{O} \cdots \text{Br}/\text{Br} \cdots \text{O}$, (m) $\text{C} \cdots \text{Cl}/\text{Cl} \cdots \text{C}$ and (n) $\text{O} \cdots \text{Cl}/\text{Cl} \cdots \text{O}$ interactions. The d_i and d_e values are the closest internal and external distances (in \AA) from given points on the Hirshfeld surface.

**Figure 7**

The full two-dimensional fingerprint plots for compound (II), showing (a) all interactions, and delineated into (b) $\text{H}\cdots\text{Br/Br}\cdots\text{H}$, (c) $\text{H}\cdots\text{H}$, (d) $\text{H}\cdots\text{O/O}\cdots\text{H}$, (e) $\text{H}\cdots\text{C/C}\cdots\text{H}$, (f) $\text{C}\cdots\text{Br/Br}\cdots\text{C}$, (g) $\text{Br}\cdots\text{Br}$, (h) $\text{C}\cdots\text{O/O}\cdots\text{C}$ and (i) $\text{C}\cdots\text{C}$ interactions. The d_i and d_e values are the closest internal and external distances (in Å) from given points on the Hirshfeld surface.

$\text{Br}\cdots\text{H}$ for (II) contributing 27.5% and 36.1%, respectively, to the overall crystal packings, which are shown in Fig. 6b and Fig. 7b with the tips at $d_e + d_i = 2.95$ and 2.94 Å, respectively. The $\text{H}\cdots\text{O/O}\cdots\text{H}$ contacts (Fig. 6c and Fig. 7d) contribute 15.0% and 14.1%, and they are viewed as the pairs of spikes with the tips at $d_e + d_i = 2.08$ and 2.10 Å, respectively. The $\text{H}\cdots\text{Br/Br}\cdots\text{H}$ contacts in (I) (Fig. 6d) contribute 10.2% to the HS, and they are viewed as a pair of wings at $d_e + d_i = 2.94$ Å. The $\text{H}\cdots\text{H}$ contacts (Fig. 6e and Fig. 7c) have wide spreads of points, and are viewed at $d_e = d_i = 1.40$ Å and 1.28 Å, respectively. In the absence of $\text{C}-\text{H}\cdots\pi$ interactions, the characteristic wings of the $\text{H}\cdots\text{C/C}\cdots\text{H}$ contacts, contributing 8.1% and 13.9% to the overall crystal packings are seen in Fig. 6f and Fig. 7e with the tips at $d_e + d_i = 3.24$ and 2.78 Å, respectively. The tiny spikes of $\text{Cl}\cdots\text{Br/Br}\cdots\text{Cl}$ for (I) (Fig. 6g), which contribute 7.2% to the HS are seen at $d_e + d_i = 3.68$ Å. The $\text{C}\cdots\text{C}$ contacts (Fig. 6h and Fig. 7f), contributing 6.5% and 0.3%, have arrow-shaped distributions of points at $d_e = d_i = 1.66$ Å for (I). The symmetrical pairs of $\text{C}\cdots\text{Br/Br}\cdots\text{C}$ contacts (Fig. 6i and Fig. 7f) contribute 5.6% and 7.8% with the tips at $d_e + d_i = 3.48$ and 3.40 Å, respectively. The $\text{Cl}\cdots\text{Cl}$ contacts in (I) (Fig. 6j) have a bullet-shaped distribution of points with a 4.8% contribution to the HS, and the tip at $d_e = d_i = 1.86$ Å. The $\text{Br}\cdots\text{Br}$ contacts (Fig. 6k and Fig. 7g) contribute 2.7% and 4.2% and have a needle-shaped distributions of points, $d_e = d_i = 1.74$ and 1.88 Å, respectively. The $\text{O}\cdots\text{Br/Br}\cdots\text{O}$ interactions in (I) (Fig. 6l) contribute 2.5% to the HS and have the tips at $d_e + d_i = 3.60$ Å. Finally, the $\text{C}\cdots\text{Cl/Cl}\cdots\text{C}$ (Fig. 6m), $\text{O}\cdots\text{Cl/Cl}\cdots\text{O}$ (Fig. 6n) and $\text{C}\cdots\text{O}/$

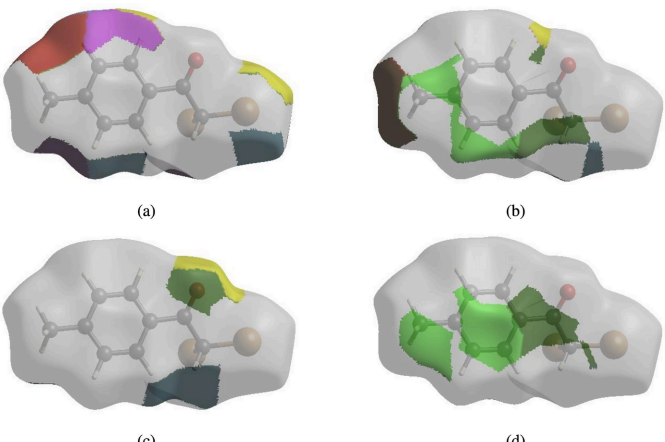
**Figure 8**

The Hirshfeld surface representations of contact patches for compound (I) plotted onto the surface for (a) $\text{H}\cdots\text{Cl/Cl}\cdots\text{H}$, (b) $\text{H}\cdots\text{O/O}\cdots\text{H}$, (c) $\text{H}\cdots\text{Br/Br}\cdots\text{H}$ and (d) $\text{H}\cdots\text{H}$ interactions.

$\text{O}\cdots\text{C}$ (Fig. 7h) contacts with contributions of 0.4%, 0.2% and 0.7%, respectively, have very low densities.

The nearest neighbour coordination environment of a molecule can be determined from the colour patches on the HS based on how close to other molecules they are. The Hirshfeld surface representations of contact patches plotted onto the surfaces are shown for the $\text{H}\cdots\text{Cl/Cl}\cdots\text{H}$, $\text{H}\cdots\text{O/O}\cdots\text{H}$, $\text{H}\cdots\text{Br/Br}\cdots\text{H}$, $\text{H}\cdots\text{H}$ and $\text{H}\cdots\text{C/C}\cdots\text{H}$ interactions in Fig. 8a–d and Fig. 9a–d for both compounds (I) and (II), respectively.

The Hirshfeld surface analyses confirms the importance of H-atom contacts in establishing the packings. The large number of $\text{H}\cdots\text{Cl/Cl}\cdots\text{H}$, $\text{H}\cdots\text{O/O}\cdots\text{H}$, $\text{H}\cdots\text{Br/Br}\cdots\text{H}$, $\text{H}\cdots\text{H}$ and $\text{H}\cdots\text{C/C}\cdots\text{H}$ interactions suggest that van der Waals interactions and hydrogen bonding play the major roles in the crystal packing (Hathwar *et al.*, 2015).

**Figure 9**

The Hirshfeld surface representations of contact patches for compound (II) plotted onto the surface for (a) $\text{H}\cdots\text{Br/Br}\cdots\text{H}$, (b) $\text{H}\cdots\text{H}$, (c) $\text{H}\cdots\text{O/O}\cdots\text{H}$ and (d) $\text{H}\cdots\text{C/C}\cdots\text{H}$ interactions.

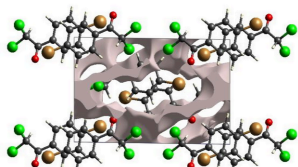
Table 5
Experimental details.

	(I)	(II)
Crystal data		
Chemical formula	C ₈ H ₅ BrCl ₂ O	C ₉ H ₈ Br ₂ O
M _r	267.93	291.97
Crystal system, space group	Triclinic, P $\bar{1}$	Monoclinic, P2 ₁ /c
Temperature (K)	100	100
a, b, c (Å)	7.0317 (1), 9.78938 (18), 14.4440 (3)	6.6243 (1), 9.9574 (1), 14.3804 (2)
α , β , γ (°)	87.5944 (15), 84.7254 (13), 72.0372 (14)	90, 92.520 (1), 90
V (Å ³)	941.70 (3)	947.63 (2)
Z	4	4
Radiation type	Cu K α	Cu K α
μ (mm ⁻¹)	10.75	10.43
Crystal size (mm)	0.35 × 0.21 × 0.16	0.22 × 0.16 × 0.12
Data collection		
Diffractometer	XtaLAB Synergy, Dualflex, HyPix	XtaLAB Synergy, Dualflex, HyPix
Absorption correction	Gaussian (CrysAlis PRO; Rigaku OD, 2024)	Gaussian (CrysAlisPr; Rigaku OD, 2024)
T _{min} , T _{max}	0.169, 1.000	0.198, 0.680
No. of measured, independent and observed [I > 2σ(I)] reflections	24768, 4027, 3992	12954, 2075, 2046
R _{int}	0.041	0.031
(sin θ/λ) _{max} (Å ⁻¹)	0.638	0.640
Refinement		
R[F ² > 2σ(F ²)], wR(F ²), S	0.031, 0.085, 1.10	0.027, 0.071, 1.08
No. of reflections	4027	2075
No. of parameters	218	111
H-atom treatment	H-atom parameters constrained	H-atom parameters constrained
Δρ _{max} , Δρ _{min} (e Å ⁻³)	0.63, -0.71	0.61, -0.51

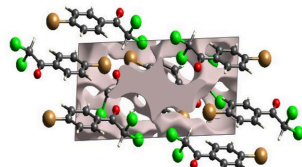
Computer programs: CrysAlis PRO (Rigaku OD, 2024), SHELLXT2018/2 (Sheldrick, 2015a), SHELLXL2018/3 (Sheldrick, 2015b) and OLEX2 (Dolomanov *et al.*, 2009).

5. Crystal voids

The strength of the crystal packing is important for determining the response to an applied mechanical force. If the crystal packing results in significant voids, the molecules are not tightly packed and a small amount of applied external mechanical force may easily break the crystal. To check the mechanical stability of the crystal, a void analysis was performed by adding up the electron densities of the spherically symmetric atoms contained in the asymmetric unit (Turner *et al.*, 2011). The void surface is defined as an isosurface of the procrystal electron density and is calculated for the whole unit cell where the void surface meets the boundary of the unit cell and capping faces are generated to create an enclosed volume. The volumes of the crystal voids (Figs. 10 and 11) and the percentages of free space in the unit cells were calculated to be 111.55 Å³ and 12.27%, respectively, for (I) and 63.37 Å³ and 6.69% for (I). Thus, the crystal packings appear compact and the mechanical stability should be substantial.



(a)

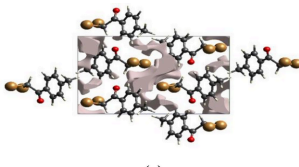


(b)

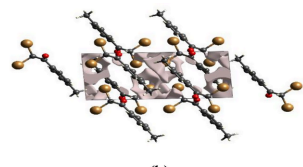
Figure 10
Graphical views of voids in the crystal packing of compound (I) along the (a) *a*-axis and (b) *b*-axis directions.

6. Synthesis and crystallization

To a solution of 3-(4-bromophenyl)-2,2-dichloro-3-oxopropanal or 2,2-dibromo-3-oxo-3-(*p*-tolyl)propanal (1.00 mmol) in 20 ml of chloroform was added diaminofurazan (1.00 mmol) and the mixture was refluxed at 353 K for 1 h. Then, the chloroform was evacuated under vacuum; the remaining reaction mass was added to 20 ml of diethyl ether. The precipitated *N*-(4-amino-1,2,5-oxadiazol-3-yl)formamide (yield: 82 or 77%) was filtered off. The 1-(4-bromophenyl)-2,2-dichloroethan-1-one (I) or 2,2-dibromo-1-(*p*-tolyl)ethan-1-one (II) was isolated (yield: 79 or 75%) from the filtrate. (I): ¹H NMR (300 MHz, DMSO-*d*₆): δ = 8.20 (*d*, 2H), 7.89 (*s*, 1H), 7.44 (*d*, 2H). ¹³C NMR (151 MHz, CDCl₃) δ = 185.60, 145.87, 129.87, 129.65, 128.75, 67.84. (II): ¹H NMR (300 MHz, DMSO-*d*₆): δ = 8.21 (*d*, 2H), 7.75 (*s*, 1H), 7.30 (*d*, 2H), 2.35 (*s*, 3H). ¹³C NMR (151 MHz, CDCl₃) δ = 184.95, 141.25, 131.25, 129.49, 129.30, 51.79, 21.85. *N*-(4-Amino-1,2,5-oxadiazol-3-yl)formamide: ¹H NMR (300 MHz, DMSO-*d*₆): δ = 10.40 (*bd*, 1H, NH), 8.75 (*bd*, 1H, CHO), 6.11 (*bs*, 2H, NH₂).



(a)



(b)

Figure 11
Graphical views of voids in the crystal packing of compound (II) along the (a) *a*-axis and (b) *b*-axis directions.

7. Refinement

Crystal data, data collection and structure refinement details are summarized in Table 5. The C-bond hydrogen-atom positions were calculated geometrically at distances of 1.00 Å (for methine CH), 0.95 Å (for aromatic CH) and 0.98 Å (for CH₃) and refined using a riding model by applying the constraint of $U_{\text{iso}}(\text{H}) = k \times U_{\text{eq}}(\text{C})$, where $k = 1.5$ for methyl H atoms and $k = 1.2$ for the other H atoms.

Acknowledgements

Crystal structure determination was performed in the Department of Structural Studies of Zelinsky Institute of Organic Chemistry, Moscow. This work has been supported by the Baku State University, Azerbaijan Medical University and Khazar University in Azerbaijan. The author's contributions are as follows. Conceptualization, AVG, TH and ANB; synthesis, AVG and FIG; X-ray analysis, AIS; writing (review and editing of the manuscript) AVG and TH; funding acquisition, AVG, KIH and TAJ; supervision, AVG, TH and ANB.

References

- Dolomanov, O. V., Bourhis, L. J., Gildea, R. J., Howard, J. A. K. & Puschmann, H. (2009). *J. Appl. Cryst.* **42**, 339–341.
- Erian, A. W., Sherif, S. M. & Gaber, H. M. (2003). *Molecules*, **8**, 793–865.
- Gurbanov, A. V., Kuznetsov, M. L., Karmakar, A., Aliyeva, V. A., Mahmudov, K. T. & Pombeiro, A. J. L. (2022). *Dalton Trans.* **51**, 1019–1031.
- Guseinov, F. I., Pistsov, M. F., Malinnikov, V. M., Lavrova, O. M., Movsumzade, E. M. & Kustov, L. M. (2020). *Mendeleev Commun.* **30**, 674–675.
- Guseinov, F. I., Pistsov, M. F., Movsumzade, E. M., Kustov, L. M., Tafeenko, V. A., Chernyshev, V. V., Gurbanov, A. V., Mahmudov, K. T. & Pombeiro, A. (2017). *Crystals*, **7**, 327.
- Guseinov, F. N., Burangulova, R. N., Mukhamedzyanova, E. F., Strunin, B. P., Sinyashin, O. G., Litvinov, I. A. & Gubaiddullin, A. T. (2006). *Chem. Heterocycl. Compd.* **42**, 943–947.
- Guseinov, F. N., Ovsyannikov, V. O., Shuvalova, E. V., Kustov, L. M., Kobrakov, K. I., Samigullina, A. I. & Mahmudov, K. T. (2024). *New J. Chem.* **48**, 12869–12872.
- Hathwar, V. R., Sist, M., Jørgensen, M. R. V., Mamakhel, A. H., Wang, X., Hoffmann, C. M., Sugimoto, K., Overgaard, J. & Iversen, B. B. (2015). *IUCrJ*, **2**, 563–574.
- Hirshfeld, H. L. (1977). *Theor. Chim. Acta*, **44**, 129–138.
- Jayatilaka, D., Grimwood, D. J., Lee, A., Lemay, A., Russel, A. J., Taylor, C., Wolff, S. K., Cassam-Chenai, P. & Whitton, A. (2005). *TONTO - A System for Computational Chemistry*. Available at: <http://hirshfeldsurface.net/>.
- Khalilov, A. N., Cisterna, J., Cárdenas, A., Tuzun, B., Erkan, S., Gurbanov, A. V. & Brito, I. (2024). *J. Mol. Struct.* **1313**, 138652.
- Ma, Z., Mahmudov, K. T., Aliyeva, V. A., Gurbanov, A. V., Guedes da Silva, M. F. C. & Pombeiro, A. J. L. (2021). *Coord. Chem. Rev.* **437**, 213859.
- Mahmoudi, G., Zaręba, J. K., Gurbanov, A. V., Bauzá, A., Zubkov, F. I., Kubicki, M., Stilinović, V., Kinzhybalo, V. & Frontera, A. (2017). *Eur. J. Inorg. Chem.* pp. 4763–4772.
- McKinnon, J. J., Jayatilaka, D. & Spackman, M. A. (2007). *Chem. Commun.* pp. 3814–3816.
- Mizar, A., Guedes da Silva, M. F. C., Kopylovich, M. N., Mukherjee, S., Mahmudov, K. T. & Pombeiro, A. J. L. (2012). *Eur. J. Inorg. Chem.* **2012**, 2305–2313.
- Rigaku OD (2024). *CrysAlis PRO*. Rigaku Oxford Diffraction, Yarnton, England.
- Sheldrick, G. M. (2015a). *Acta Cryst. A* **71**, 3–8.
- Sheldrick, G. M. (2015b). *Acta Cryst. C* **71**, 3–8.
- Spackman, M. A. & Jayatilaka, D. (2009). *CrystEngComm*, **11**, 19–32.
- Spackman, M. A., McKinnon, J. J. & Jayatilaka, D. (2008). *CrystEngComm*, **10**, 377–388.
- Spackman, P. R., Turner, M. J., McKinnon, J. J., Wolff, S. K., Grimwood, D. J., Jayatilaka, D. & Spackman, M. A. (2021). *J. Appl. Cryst.* **54**, 1006–1011.
- Turner, M. J., McKinnon, J. J., Jayatilaka, D. & Spackman, M. A. (2011). *CrystEngComm*, **13**, 1804–1813.
- Venkatesan, P., Thamotharan, S., Ilangoan, A., Liang, H. & Sundius, T. (2016). *Spectrochim. Acta A Mol. Biomol. Spectrosc.* **153**, 625–636.

supporting information

Acta Cryst. (2025). E81, 120-126 [https://doi.org/10.1107/S205698902500012X]

Syntheses, crystal structures, Hirshfeld surface analyses and crystal voids of 1-(4-bromophenyl)-2,2-dichloroethan-1-one and 2,2-dibromo-1-(*p*-tolyl)-ethan-1-one

Atash V. Gurbanov, Firudin I. Guseinov, Aida I. Samigullina, Tuncer Hökelek, Khudayar I. Hasanov, Tahir A. Javadzade and Alebel N. Belay

Computing details

1-(4-Bromophenyl)-2,2-dichloroethan-1-one (I)

Crystal data

C ₈ H ₅ BrCl ₂ O	Z = 4
M _r = 267.93	F(000) = 520
Triclinic, P $\bar{1}$	D _x = 1.890 Mg m ⁻³
a = 7.0317 (1) Å	Cu K α radiation, λ = 1.54184 Å
b = 9.78938 (18) Å	Cell parameters from 19038 reflections
c = 14.4440 (3) Å	θ = 4.7–79.0°
α = 87.5944 (15)°	μ = 10.75 mm ⁻¹
β = 84.7254 (13)°	T = 100 K
γ = 72.0372 (14)°	Prism, colorless
V = 941.70 (3) Å ³	0.35 × 0.21 × 0.16 mm

Data collection

XtaLAB Synergy, Dualflex, HyPix	T_{\min} = 0.169, T_{\max} = 1.000
diffractometer	24768 measured reflections
Radiation source: micro-focus sealed X-ray	4027 independent reflections
tube, PhotonJet (Cu) X-ray Source	3992 reflections with $I > 2\sigma(I)$
Mirror monochromator	R_{int} = 0.041
Detector resolution: 10.0000 pixels mm ⁻¹	θ_{\max} = 79.7°, θ_{\min} = 3.1°
ω scans	h = -8→8
Absorption correction: gaussian	k = -12→12
(CrysAlisPro; Rigaku OD, 2024)	l = -18→18

Refinement

Refinement on F^2	Secondary atom site location: difference Fourier
Least-squares matrix: full	map
$R[F^2 > 2\sigma(F^2)]$ = 0.031	Hydrogen site location: inferred from
wR(F^2) = 0.085	neighbouring sites
S = 1.10	H-atom parameters constrained
4027 reflections	$w = 1/[\sigma^2(F_o^2) + (0.048P)^2 + 1.1375P]$
218 parameters	where $P = (F_o^2 + 2F_c^2)/3$
0 restraints	$(\Delta/\sigma)_{\max} = 0.003$
Primary atom site location: dual	$\Delta\rho_{\max} = 0.63 \text{ e } \text{\AA}^{-3}$
	$\Delta\rho_{\min} = -0.70 \text{ e } \text{\AA}^{-3}$

Extinction correction: *SHELXL2018/3*
 (Sheldrick, 2015b),
 $F_c^* = k F_c [1 + 0.001 x F_c^2 \lambda^3 / \sin(2\theta)]^{-1/4}$
 Extinction coefficient: 0.0022 (2)

Special details

Geometry. All esds (except the esd in the dihedral angle between two l.s. planes) are estimated using the full covariance matrix. The cell esds are taken into account individually in the estimation of esds in distances, angles and torsion angles; correlations between esds in cell parameters are only used when they are defined by crystal symmetry. An approximate (isotropic) treatment of cell esds is used for estimating esds involving l.s. planes.

Fractional atomic coordinates and isotropic or equivalent isotropic displacement parameters (\AA^2)

	<i>x</i>	<i>y</i>	<i>z</i>	$U_{\text{iso}}^*/U_{\text{eq}}$
Br6A	0.81615 (4)	0.56770 (3)	0.32820 (2)	0.02069 (10)
Cl1A	0.33348 (10)	0.55329 (7)	0.89875 (4)	0.02549 (15)
Cl2A	0.74935 (10)	0.53706 (8)	0.84399 (4)	0.02822 (15)
O2A	0.3354 (3)	0.7709 (2)	0.75703 (14)	0.0284 (4)
C1A	0.5180 (4)	0.5343 (3)	0.80452 (16)	0.0175 (4)
H1A	0.538721	0.440813	0.773449	0.021*
C2A	0.4551 (4)	0.6576 (3)	0.73301 (17)	0.0175 (4)
C3A	0.5482 (3)	0.6324 (2)	0.63618 (16)	0.0149 (4)
C4A	0.4938 (4)	0.7454 (3)	0.57111 (18)	0.0191 (5)
H4A	0.402128	0.835143	0.590281	0.023*
C5A	0.5718 (4)	0.7276 (3)	0.47965 (18)	0.0194 (5)
H5A	0.533876	0.803928	0.435599	0.023*
C6A	0.7077 (3)	0.5952 (3)	0.45312 (16)	0.0161 (4)
C7A	0.7639 (3)	0.4816 (2)	0.51561 (16)	0.0156 (4)
H7A	0.856155	0.392344	0.495928	0.019*
C8A	0.6835 (3)	0.4999 (2)	0.60758 (16)	0.0141 (4)
H8A	0.720183	0.422604	0.651044	0.017*
Br6B	0.76334 (4)	0.85069 (3)	1.16685 (2)	0.02310 (10)
Cl1B	1.01787 (9)	1.10238 (6)	0.60398 (4)	0.02204 (14)
Cl2B	0.80524 (11)	0.89180 (7)	0.64724 (5)	0.03046 (16)
O2B	0.7017 (3)	1.21469 (19)	0.74989 (12)	0.0218 (4)
C1B	0.9394 (4)	0.9975 (2)	0.69302 (16)	0.0170 (4)
H1B	1.059740	0.932687	0.721540	0.020*
C2B	0.7983 (3)	1.0930 (2)	0.76903 (16)	0.0152 (4)
C3B	0.7895 (3)	1.0296 (2)	0.86393 (16)	0.0147 (4)
C4B	0.7014 (4)	1.1233 (3)	0.93713 (17)	0.0180 (5)
H4B	0.646312	1.223144	0.924605	0.022*
C5B	0.6938 (4)	1.0718 (3)	1.02798 (17)	0.0204 (5)
H5B	0.636309	1.135395	1.078017	0.024*
C6B	0.7723 (4)	0.9248 (3)	1.04401 (16)	0.0177 (4)
C7B	0.8588 (4)	0.8292 (3)	0.97239 (18)	0.0207 (5)
H7B	0.910242	0.729156	0.985011	0.025*
C8B	0.8688 (4)	0.8826 (3)	0.88192 (17)	0.0192 (5)
H8B	0.929655	0.818923	0.832274	0.023*

Atomic displacement parameters (\AA^2)

	U^{11}	U^{22}	U^{33}	U^{12}	U^{13}	U^{23}
Br6A	0.02097 (15)	0.03124 (16)	0.01216 (14)	-0.01176 (11)	-0.00107 (9)	0.00224 (10)
Cl1A	0.0275 (3)	0.0262 (3)	0.0176 (3)	-0.0025 (2)	0.0063 (2)	-0.0035 (2)
Cl2A	0.0248 (3)	0.0411 (4)	0.0190 (3)	-0.0092 (3)	-0.0068 (2)	0.0002 (2)
O2A	0.0356 (10)	0.0181 (9)	0.0214 (9)	0.0064 (8)	0.0004 (8)	-0.0053 (7)
C1A	0.0193 (11)	0.0176 (11)	0.0118 (10)	-0.0005 (8)	0.0017 (8)	-0.0028 (8)
C2A	0.0202 (11)	0.0148 (10)	0.0164 (11)	-0.0026 (8)	-0.0035 (9)	-0.0028 (8)
C3A	0.0160 (10)	0.0132 (10)	0.0159 (10)	-0.0046 (8)	-0.0028 (8)	-0.0025 (8)
C4A	0.0211 (11)	0.0152 (10)	0.0208 (12)	-0.0046 (9)	-0.0036 (9)	-0.0002 (9)
C5A	0.0214 (11)	0.0163 (11)	0.0207 (12)	-0.0053 (9)	-0.0054 (9)	0.0035 (9)
C6A	0.0163 (10)	0.0218 (11)	0.0127 (10)	-0.0098 (9)	-0.0008 (8)	-0.0007 (9)
C7A	0.0150 (10)	0.0170 (10)	0.0148 (11)	-0.0044 (8)	-0.0019 (8)	-0.0010 (8)
C8A	0.0138 (10)	0.0144 (10)	0.0141 (10)	-0.0039 (8)	-0.0027 (8)	0.0000 (8)
Br6B	0.02356 (16)	0.03377 (17)	0.01465 (15)	-0.01308 (11)	-0.00342 (10)	0.00666 (10)
Cl1B	0.0306 (3)	0.0205 (3)	0.0144 (3)	-0.0082 (2)	0.0030 (2)	0.0001 (2)
Cl2B	0.0472 (4)	0.0293 (3)	0.0233 (3)	-0.0233 (3)	-0.0023 (3)	-0.0082 (2)
O2B	0.0258 (9)	0.0166 (8)	0.0184 (8)	-0.0011 (7)	0.0011 (7)	0.0020 (7)
C1B	0.0239 (11)	0.0152 (10)	0.0119 (10)	-0.0061 (9)	-0.0008 (9)	-0.0012 (8)
C2B	0.0165 (10)	0.0146 (10)	0.0147 (10)	-0.0046 (8)	-0.0020 (8)	-0.0020 (8)
C3B	0.0140 (10)	0.0165 (10)	0.0143 (10)	-0.0053 (8)	-0.0024 (8)	0.0001 (8)
C4B	0.0219 (11)	0.0152 (10)	0.0181 (11)	-0.0071 (9)	-0.0018 (9)	-0.0015 (9)
C5B	0.0240 (12)	0.0225 (12)	0.0162 (11)	-0.0095 (9)	0.0004 (9)	-0.0042 (9)
C6B	0.0187 (11)	0.0250 (12)	0.0119 (10)	-0.0101 (9)	-0.0038 (8)	0.0034 (9)
C7B	0.0226 (12)	0.0182 (11)	0.0190 (12)	-0.0041 (9)	0.0000 (9)	0.0044 (9)
C8B	0.0199 (11)	0.0169 (11)	0.0172 (11)	-0.0011 (9)	0.0016 (9)	-0.0020 (9)

Geometric parameters (\AA , $^\circ$)

Br6A—C6A	1.890 (2)	Br6B—C6B	1.892 (2)
Cl1A—C1A	1.766 (2)	Cl1B—C1B	1.766 (2)
Cl2A—C1A	1.781 (3)	Cl2B—C1B	1.781 (2)
O2A—C2A	1.209 (3)	O2B—C2B	1.210 (3)
C1A—H1A	1.0000	C1B—H1B	1.0000
C1A—C2A	1.540 (3)	C1B—C2B	1.542 (3)
C2A—C3A	1.486 (3)	C2B—C3B	1.485 (3)
C3A—C4A	1.404 (3)	C3B—C4B	1.398 (3)
C3A—C8A	1.403 (3)	C3B—C8B	1.396 (3)
C4A—H4A	0.9500	C4B—H4B	0.9500
C4A—C5A	1.380 (4)	C4B—C5B	1.388 (4)
C5A—H5A	0.9500	C5B—H5B	0.9500
C5A—C6A	1.397 (3)	C5B—C6B	1.390 (4)
C6A—C7A	1.385 (3)	C6B—C7B	1.389 (3)
C7A—H7A	0.9500	C7B—H7B	0.9500
C7A—C8A	1.391 (3)	C7B—C8B	1.391 (3)
C8A—H8A	0.9500	C8B—H8B	0.9500

Br6A···Br6B ⁱ	3.4966 (4)	H5B···O2A ^{vii}	2.63
Br6A···C1A ⁱⁱ	3.554 (3)	O2A···H4A	2.50
C2A···Br6A ⁱⁱ	3.515 (3)	O2B···H1A ^v	2.18
Br6B···C2B ⁱⁱⁱ	3.504 (2)	O2B···H4B	2.52
Br6A···H1A ⁱⁱ	3.03	O2B···H8A ^v	2.47
Cl1A···O2A	2.894 (2)	C6A···C8A ⁱⁱ	3.361 (3)
Cl1B···O2B	2.901 (2)	C1A···H8A	2.61
Cl2B···C8B	3.453 (3)	C1B···H8B	2.62
Cl2B···C4A	3.251 (3)	C8A···H1A	2.63
Cl2B···H8B	2.88	C8B···H1B	2.67
O2A···C1B ^{iv}	3.166 (3)	H1A···H8A	2.06
O2B···C1A ^v	3.100 (3)	H1B···H8B	2.20
H1B···O2A ^{vi}	2.18		
Cl1A—C1A—Cl2A	110.59 (13)	Cl1B—C1B—Cl2B	110.50 (13)
Cl1A—C1A—H1A	109.1	Cl1B—C1B—H1B	109.2
Cl2A—C1A—H1A	109.1	Cl2B—C1B—H1B	109.2
C2A—C1A—Cl1A	111.28 (16)	C2B—C1B—Cl1B	111.22 (16)
C2A—C1A—Cl2A	107.49 (17)	C2B—C1B—Cl2B	107.41 (16)
C2A—C1A—H1A	109.1	C2B—C1B—H1B	109.2
O2A—C2A—C1A	119.8 (2)	O2B—C2B—C1B	119.7 (2)
O2A—C2A—C3A	122.4 (2)	O2B—C2B—C3B	122.9 (2)
C3A—C2A—C1A	117.9 (2)	C3B—C2B—C1B	117.4 (2)
C4A—C3A—C2A	118.0 (2)	C4B—C3B—C2B	117.6 (2)
C8A—C3A—C2A	122.5 (2)	C8B—C3B—C2B	122.5 (2)
C8A—C3A—C4A	119.5 (2)	C8B—C3B—C4B	119.9 (2)
C3A—C4A—H4A	119.6	C3B—C4B—H4B	119.7
C5A—C4A—C3A	120.8 (2)	C5B—C4B—C3B	120.6 (2)
C5A—C4A—H4A	119.6	C5B—C4B—H4B	119.7
C4A—C5A—H5A	120.7	C4B—C5B—H5B	120.8
C4A—C5A—C6A	118.7 (2)	C4B—C5B—C6B	118.4 (2)
C6A—C5A—H5A	120.7	C6B—C5B—H5B	120.8
C5A—C6A—Br6A	119.57 (18)	C5B—C6B—Br6B	119.59 (18)
C7A—C6A—Br6A	118.54 (18)	C7B—C6B—Br6B	118.29 (18)
C7A—C6A—C5A	121.9 (2)	C7B—C6B—C5B	122.1 (2)
C6A—C7A—H7A	120.4	C6B—C7B—H7B	120.6
C6A—C7A—C8A	119.1 (2)	C6B—C7B—C8B	118.9 (2)
C8A—C7A—H7A	120.4	C8B—C7B—H7B	120.6
C3A—C8A—H8A	120.0	C3B—C8B—H8B	119.9
C7A—C8A—C3A	120.0 (2)	C7B—C8B—C3B	120.1 (2)
C7A—C8A—H8A	120.0	C7B—C8B—H8B	119.9
Br6A—C6A—C7A—C8A	-179.28 (17)	Br6B—C6B—C7B—C8B	-179.14 (19)
Cl1A—C1A—C2A—O2A	23.6 (3)	Cl1B—C1B—C2B—O2B	25.4 (3)
Cl1A—C1A—C2A—C3A	-157.33 (17)	Cl1B—C1B—C2B—C3B	-154.12 (17)
Cl2A—C1A—C2A—O2A	-97.6 (2)	Cl2B—C1B—C2B—O2B	-95.6 (2)
Cl2A—C1A—C2A—C3A	81.4 (2)	Cl2B—C1B—C2B—C3B	84.8 (2)
O2A—C2A—C3A—C4A	0.1 (4)	O2B—C2B—C3B—C4B	-14.4 (3)

O2A—C2A—C3A—C8A	−178.4 (2)	O2B—C2B—C3B—C8B	167.0 (2)
C1A—C2A—C3A—C4A	−178.9 (2)	C1B—C2B—C3B—C4B	165.1 (2)
C1A—C2A—C3A—C8A	2.6 (3)	C1B—C2B—C3B—C8B	−13.5 (3)
C2A—C3A—C4A—C5A	−178.6 (2)	C2B—C3B—C4B—C5B	−178.0 (2)
C2A—C3A—C8A—C7A	179.0 (2)	C2B—C3B—C8B—C7B	179.1 (2)
C3A—C4A—C5A—C6A	−0.6 (4)	C3B—C4B—C5B—C6B	−1.2 (4)
C4A—C3A—C8A—C7A	0.6 (3)	C4B—C3B—C8B—C7B	0.5 (4)
C4A—C5A—C6A—Br6A	179.75 (18)	C4B—C5B—C6B—Br6B	−179.69 (18)
C4A—C5A—C6A—C7A	0.8 (4)	C4B—C5B—C6B—C7B	0.5 (4)
C5A—C6A—C7A—C8A	−0.3 (3)	C5B—C6B—C7B—C8B	0.6 (4)
C6A—C7A—C8A—C3A	−0.4 (3)	C6B—C7B—C8B—C3B	−1.2 (4)
C8A—C3A—C4A—C5A	−0.1 (4)	C8B—C3B—C4B—C5B	0.7 (4)

Symmetry codes: (i) $x, y, z-1$; (ii) $-x+1, -y+1, -z+1$; (iii) $-x+2, -y+2, -z+2$; (iv) $x-1, y, z$; (v) $x, y+1, z$; (vi) $x+1, y, z$; (vii) $-x+1, -y+2, -z+2$.

Hydrogen-bond geometry (\AA , °)

$D-\text{H}\cdots A$	$D-\text{H}$	$\text{H}\cdots A$	$D\cdots A$	$D-\text{H}\cdots A$
C1A—H1A…O2B ^{viii}	1.00	2.18	3.100 (3)	152
C1B—H1B…O2A ^{vi}	1.00	2.18	3.166 (3)	169
C8A—H8A…O2B ^{viii}	0.95	2.47	3.374 (3)	160

Symmetry codes: (vi) $x+1, y, z$; (viii) $x, y-1, z$.

2,2-Dibromo-1-(4-methylphenyl)ethan-1-one (II)

Crystal data

$\text{C}_9\text{H}_8\text{Br}_2\text{O}$	$F(000) = 560$
$M_r = 291.97$	$D_x = 2.047 \text{ Mg m}^{-3}$
Monoclinic, $P2_1/c$	$\text{Cu } K\alpha \text{ radiation, } \lambda = 1.54184 \text{ \AA}$
$a = 6.6243 (1) \text{ \AA}$	Cell parameters from 8712 reflections
$b = 9.9574 (1) \text{ \AA}$	$\theta = 4.4\text{--}80.2^\circ$
$c = 14.3804 (2) \text{ \AA}$	$\mu = 10.43 \text{ mm}^{-1}$
$\beta = 92.520 (1)^\circ$	$T = 100 \text{ K}$
$V = 947.63 (2) \text{ \AA}^3$	Prism, colorless
$Z = 4$	$0.22 \times 0.16 \times 0.12 \text{ mm}$

Data collection

XtaLAB Synergy, Dualflex, HyPix diffractometer	$T_{\min} = 0.198, T_{\max} = 0.680$
Radiation source: micro-focus sealed X-ray tube, PhotonJet (Cu) X-ray Source	12954 measured reflections
Mirror monochromator	2075 independent reflections
Detector resolution: 10.0000 pixels mm^{-1}	2046 reflections with $I > 2\sigma(I)$
ω scans	$R_{\text{int}} = 0.031$
Absorption correction: gaussian (CrysAlisPr; Rigaku OD, 2024)	$\theta_{\max} = 80.6^\circ, \theta_{\min} = 5.4^\circ$
	$h = -8 \rightarrow 6$
	$k = -12 \rightarrow 12$
	$l = -18 \rightarrow 18$

Refinement

Refinement on F^2	$S = 1.08$
Least-squares matrix: full	2075 reflections
$R[F^2 > 2\sigma(F^2)] = 0.027$	111 parameters
$wR(F^2) = 0.071$	0 restraints

Primary atom site location: dual
 Secondary atom site location: difference Fourier map
 Hydrogen site location: inferred from neighbouring sites
 H-atom parameters constrained
 $w = 1/[\sigma^2(F_o^2) + (0.0353P)^2 + 1.8407P]$
 where $P = (F_o^2 + 2F_c^2)/3$

$(\Delta/\sigma)_{\max} = 0.001$
 $\Delta\rho_{\max} = 0.61 \text{ e } \text{\AA}^{-3}$
 $\Delta\rho_{\min} = -0.51 \text{ e } \text{\AA}^{-3}$
 Extinction correction: *SHELXL2018/3*
 (Sheldrick, 2015b),
 $F_c^* = k F_c [1 + 0.001 x F_c^2 \lambda^3 / \sin(2\theta)]^{-1/4}$
 Extinction coefficient: 0.00143 (13)

Special details

Geometry. All esds (except the esd in the dihedral angle between two l.s. planes) are estimated using the full covariance matrix. The cell esds are taken into account individually in the estimation of esds in distances, angles and torsion angles; correlations between esds in cell parameters are only used when they are defined by crystal symmetry. An approximate (isotropic) treatment of cell esds is used for estimating esds involving l.s. planes.

Fractional atomic coordinates and isotropic or equivalent isotropic displacement parameters (\AA^2)

	<i>x</i>	<i>y</i>	<i>z</i>	$U_{\text{iso}}^*/U_{\text{eq}}$
Br1	1.23695 (4)	0.66709 (3)	0.63489 (2)	0.01960 (11)
Br2	0.77764 (4)	0.64644 (3)	0.55958 (2)	0.02528 (12)
O2	0.9676 (3)	0.8317 (2)	0.75385 (16)	0.0251 (4)
C1	0.9651 (4)	0.6269 (3)	0.66762 (18)	0.0169 (5)
H1	0.959154	0.532581	0.691175	0.020*
C2	0.8893 (4)	0.7229 (3)	0.74202 (18)	0.0163 (5)
C3	0.7113 (4)	0.6791 (3)	0.79372 (19)	0.0181 (5)
C4	0.5987 (4)	0.7784 (3)	0.83659 (18)	0.0186 (5)
H4	0.639502	0.869684	0.833713	0.022*
C5	0.4273 (4)	0.7438 (3)	0.88335 (18)	0.0195 (5)
H5	0.350118	0.812055	0.911211	0.023*
C6	0.3669 (4)	0.6097 (3)	0.88997 (18)	0.0185 (5)
C7	0.4849 (4)	0.5111 (3)	0.84988 (19)	0.0195 (5)
H7	0.449098	0.419262	0.856196	0.023*
C8	0.6538 (4)	0.5447 (3)	0.80095 (18)	0.0186 (5)
H8	0.730070	0.476472	0.772465	0.022*
C9	0.1787 (4)	0.5707 (3)	0.9386 (2)	0.0236 (6)
H9A	0.216416	0.531296	0.999369	0.035*
H9B	0.102049	0.504843	0.900725	0.035*
H9C	0.095251	0.650586	0.947391	0.035*

Atomic displacement parameters (\AA^2)

	U^{11}	U^{22}	U^{33}	U^{12}	U^{13}	U^{23}
Br1	0.01651 (16)	0.02134 (17)	0.02127 (17)	-0.00045 (9)	0.00428 (10)	0.00094 (10)
Br2	0.02045 (17)	0.03458 (19)	0.02068 (17)	-0.00176 (11)	-0.00073 (11)	-0.00414 (11)
O2	0.0244 (10)	0.0201 (10)	0.0314 (11)	-0.0065 (8)	0.0095 (8)	-0.0060 (8)
C1	0.0136 (11)	0.0193 (12)	0.0179 (12)	-0.0003 (9)	0.0025 (9)	0.0003 (10)
C2	0.0161 (11)	0.0152 (12)	0.0176 (11)	-0.0002 (9)	0.0015 (9)	0.0014 (9)
C3	0.0164 (12)	0.0177 (12)	0.0203 (12)	-0.0002 (10)	0.0010 (10)	0.0007 (10)
C4	0.0190 (12)	0.0169 (12)	0.0198 (12)	-0.0005 (9)	-0.0001 (9)	0.0001 (10)
C5	0.0201 (12)	0.0218 (13)	0.0167 (11)	0.0045 (10)	0.0022 (9)	-0.0031 (10)

C6	0.0176 (12)	0.0248 (13)	0.0132 (11)	-0.0005 (10)	0.0013 (9)	-0.0001 (10)
C7	0.0182 (12)	0.0193 (12)	0.0210 (12)	-0.0011 (10)	0.0007 (10)	0.0008 (10)
C8	0.0187 (12)	0.0177 (13)	0.0196 (12)	0.0005 (9)	0.0030 (9)	0.0008 (10)
C9	0.0199 (12)	0.0287 (15)	0.0228 (13)	-0.0025 (11)	0.0053 (10)	-0.0001 (11)

Geometric parameters (\AA , $^\circ$)

Br1—C1	1.923 (3)	C5—H5	0.9500
Br2—C1	1.955 (3)	C5—C6	1.398 (4)
O2—C2	1.210 (3)	C6—C7	1.396 (4)
C1—H1	1.0000	C6—C9	1.507 (4)
C1—C2	1.535 (4)	C7—H7	0.9500
C2—C3	1.487 (4)	C7—C8	1.389 (4)
C3—C4	1.398 (4)	C8—H8	0.9500
C3—C8	1.396 (4)	C9—H9A	0.9800
C4—H4	0.9500	C9—H9B	0.9800
C4—C5	1.388 (4)	C9—H9C	0.9800
Br1···O2	3.011 (2)	H8···O2 ⁱⁱ	2.51
C4···Br2 ⁱ	3.452 (3)	C1···H8	2.67
C5···Br2 ⁱ	3.534 (3)	C8···H1	2.62
C1···O2 ⁱⁱ	3.173 (4)	H1···H8	2.03
O2···H4	2.53	H5···H9C	2.40
H1···O2 ⁱⁱ	2.20		
Br1—C1—Br2	110.71 (13)	C6—C5—H5	119.6
Br1—C1—H1	109.2	C5—C6—C9	121.5 (2)
Br2—C1—H1	109.2	C7—C6—C5	118.4 (2)
C2—C1—Br1	112.31 (18)	C7—C6—C9	120.0 (3)
C2—C1—Br2	106.03 (17)	C6—C7—H7	119.4
C2—C1—H1	109.2	C8—C7—C6	121.2 (3)
O2—C2—C1	120.3 (2)	C8—C7—H7	119.4
O2—C2—C3	122.5 (2)	C3—C8—H8	120.1
C3—C2—C1	117.2 (2)	C7—C8—C3	119.8 (3)
C4—C3—C2	117.6 (2)	C7—C8—H8	120.1
C8—C3—C2	122.9 (2)	C6—C9—H9A	109.5
C8—C3—C4	119.5 (2)	C6—C9—H9B	109.5
C3—C4—H4	119.9	C6—C9—H9C	109.5
C5—C4—C3	120.1 (3)	H9A—C9—H9B	109.5
C5—C4—H4	119.9	H9A—C9—H9C	109.5
C4—C5—H5	119.6	H9B—C9—H9C	109.5
C4—C5—C6	120.9 (2)		
Br1—C1—C2—O2	21.6 (3)	C2—C3—C8—C7	-179.6 (2)
Br1—C1—C2—C3	-161.77 (18)	C3—C4—C5—C6	1.3 (4)
Br2—C1—C2—O2	-99.5 (3)	C4—C3—C8—C7	0.5 (4)
Br2—C1—C2—C3	77.2 (2)	C4—C5—C6—C7	1.1 (4)
O2—C2—C3—C4	18.2 (4)	C4—C5—C6—C9	-178.6 (2)

O2—C2—C3—C8	−161.7 (3)	C5—C6—C7—C8	−2.8 (4)
C1—C2—C3—C4	−158.4 (2)	C6—C7—C8—C3	2.0 (4)
C1—C2—C3—C8	21.7 (4)	C8—C3—C4—C5	−2.1 (4)
C2—C3—C4—C5	178.0 (2)	C9—C6—C7—C8	177.0 (2)

Symmetry codes: (i) $x, -y+3/2, z+1/2$; (ii) $-x+2, y-1/2, -z+3/2$.

Hydrogen-bond geometry (\AA , °)

$D\text{—H}\cdots A$	$D\text{—H}$	$\text{H}\cdots A$	$D\cdots A$	$D\text{—H}\cdots A$
C1—H1···O2 ⁱⁱ	1.00	2.20	3.173 (4)	165
C8—H8···O2 ⁱⁱ	0.95	2.51	3.403 (3)	157

Symmetry code: (ii) $-x+2, y-1/2, -z+3/2$.